Published in final edited form as:

*Cancer Prev Res (Phila)*. 2016 September ; 9(9): 721–731. doi:10.1158/1940-6207.CAPR-16-0095.

# Celecoxib alters the intestinal microbiota and metabolome in association with reducing polyp burden

**David C. Montrose**[1], **Xi Kathy Zhou**[2], **Erin M. McNally**[1], **Erika Sue**[1], **Rhonda K. Yantiss**[3], **Steven S. Gross**[4], **Nitai D. Leve**[2], **Edward D. Karoly**[5], **Chen S. Suen**[6], **Lilan Ling**[7], **Robert Benezra**[8], **Eric G. Pamer**[7,9,10], and **Andrew J. Dannenberg**[1]

[1]Department of Medicine, Weill Cornell Medical College, New York, NY

[2]Department of Healthcare Policy and Research, Weill Cornell Medical College, New York, NY

[3]Department of Pathology and Laboratory Medicine, Weill Cornell Medical College, New York, NY

[4]Department of Pharmacology, Weill Cornell Medical College, New York, NY

[5]Metabolon, Inc., Durham, NC

[6]Division of Cancer Prevention, National Cancer Institute, Rockville, MD

[7]Lucille Castori Center for Microbes, Inflammation and Cancer

[8]Cancer Biology and Genetics Program

[9]Immunology Program

[10]Infectious Diseases Service, Department of Medicine, Memorial Sloan Kettering Cancer Center, New York, NY

## Abstract

Treatment with celecoxib, a selective COX-2 inhibitor, reduces formation of premalignant adenomatous polyps in the gastrointestinal tracts of humans and mice. In addition to its chemopreventive activity, celecoxib can exhibit anti-microbial activity. Differing bacterial profiles have been found in feces from colon cancer patients compared with that of normal subjects. Moreover, preclinical studies suggest that bacteria can modulate intestinal tumorigenesis by secreting specific metabolites. In the current study, we determined whether celecoxib treatment altered the luminal microbiota and metabolome in association with reducing intestinal polyp burden in mice. Administration of celecoxib for 10 weeks markedly reduced intestinal polyp burden in $APC^{Min/+}$ mice. Treatment with celecoxib also altered select luminal bacterial populations in both $APC^{Min/+}$ and wild-type mice including decreased *Lactobacillaceae* and *Bifidobacteriaceae* as well as increased *Coriobacteriaceae*. Metabolomic analysis demonstrated that celecoxib caused a strong reduction in many fecal metabolites linked to carcinogenesis including glucose, amino acids, nucleotides and lipids. Ingenuity Pathway Analysis suggested that these changes in metabolites may contribute to reduced cell proliferation. To this end, we showed

Corresponding Author: Andrew J. Dannenberg, Department of Medicine, Weill Cornell Medicine, 525 East 68th St., Room F-206, New York, NY 10065. Phone: 212-746-4403; Fax: 212-746-4885; ajdannen@med.cornell.edu.

**Disclosures:** Edward D. Karoly is an employee of Metabolon, Inc. The other authors disclosed no potential conflicts of interest.

that celecoxib reduced cell proliferation in the base of normal appearing ileal and colonic crypts of $APC^{Min/+}$ mice. Consistent with this finding, lineage tracing indicated that celecoxib treatment reduced the rate at which Lgr5-positive stem cells gave rise to differentiated cell types in the crypts. Taken together, these results demonstrate that celecoxib alters the luminal microbiota and metabolome along with reducing epithelial cell proliferation in mice. We hypothesize that these actions contribute to its chemopreventive activity.

### Keywords

celecoxib; microbiota; metabolome; prevention; stem cells

## Introduction

The mammalian intestinal tract harbors ~$10^{14}$ microorganisms which may play a role in modulating cancer development in the gastrointestinal (GI) tract (1). Data suggest that individuals with colorectal cancer (CRC) have a distinct bacterial profile compared to healthy controls (2, 3). Whether these differences are responsible for tumor initiation or growth or simply represent an epiphenomenon resulting from tumor presence is not clear. This question has been addressed in part, through the use of mouse models suggesting that microbes may modulate tumorigenesis. For example, inoculation of specific bacterial species can enhance intestinal and colonic tumor development in $APC^{Min/+}$ and $Il10^{-/-}$ mice (4-6). Furthermore, lowering bacterial abundance can reduce tumor incidence in both colitis-associated and spontaneous tumor models (7, 8). Bacteria are believed to influence intestinal tumorigenesis through multiple mechanisms including the release of key metabolites such as bile acids, short chain fatty acids and polyamines (9-13). We previously reported alterations in fecal metabolites in association with colorectal tumor growth in mice, many of which were likely to be microbe-derived (14).

Celecoxib is a selective COX-2 inhibitor that has been used as a chemopreventive agent in at-risk populations to reduce the recurrence and burden of premalignant colorectal adenomas. For example, celecoxib administration reduced polyp number in Familial Adenomatous Polyposis patients as well as recurrence of sporadic colorectal adenomas (15), (16). Importantly, the efficacy of celecoxib as a chemopreventive agent in humans was predicted by studies in $APC^{Min/+}$ mice, in which celecoxib was effective in both preventing the development of polyps and inducing their regression (17). The chemopreventive efficacy of celecoxib is believed to be a consequence of COX-2 inhibition in both humans and mice, although data from several studies suggest that celecoxib, and similar agents, exert effects through bacteria. For example, nonsteroidal anti-inflammatory drug (NSAID)-induced enteropathy can be mediated through interactions with the intestinal microbiota (18, 19). One study demonstrated that individuals who take NSAIDs have a different bacterial profile compared to those who do not take NSAIDs (20). Celecoxib also has direct antimicrobial activity, although it is not clear whether its chemopreventive action is related to its effects on microbiota or the metabolites they produce (21, 22).

In this study, we tested whether celecoxib could alter the fecal microbiota and metabolome in association with reducing intestinal tumor burden. We found that celecoxib treatment markedly reduced intestinal polyp burden in $APC^{Min/+}$ mice. Drug administration altered bacterial populations in both ileal content and feces. Subsequent metabolomic analysis demonstrated that celecoxib reduced a large number of pro-proliferative metabolites in the GI tract, and administration of this agent resulted in reduced proliferation of normal intestinal crypt stem cells. Taken together, these results suggest that celecoxib may exert its chemopreventive effects, in part, through effects on the luminal microbiota and metabolome.

## Materials and Methods

### Mouse treatments and sample collection

Male $APC^{Min/+}$ and wild-type (WT) mice from the same colony were obtained from The Jackson Laboratory at 4 weeks of age and placed on AIN-93G purified diet (Research Diets). In order to equilibrate the microbiota across mice by microbial exchange, 2 mice of each genotype were housed together until 6 weeks of age. At 6 weeks of age, feces was collected from individual mice and snap frozen in liquid nitrogen and stored at -80°C until metabolomic and bacterial analyses were carried out. After the initial fecal collections, $APC^{Min/+}$ and WT mice were individually housed and either continued on AIN-93G purified diet or given the same diet supplemented with 1000 ppm celecoxib for 10 weeks. Feces were collected again at 11 and 16 weeks of age. All mice were sacrificed at 16 weeks of age at which time ileal content was collected and snap-frozen then intestines were flushed with ice-cold phosphate buffered saline, cut open longitudinally and formalin fixed for quantification of polyp burden. This experimental design is shown in Figure 1A. Intestines were stained with methylene blue and tumor number and size were enumerated in whole mounts under a dissecting microscope using a ruler capable of discerning size differences of 0.5mm to determine tumor size then Swiss-rolled and paraffin embedded as previously described (14). All animal studies were approved by the Institutional Animal Care and Use Committee at Weill Cornell Medical College.

### Bacterial DNA extraction

Briefly, DNA extraction was carried out by phenol chloroform extraction with mechanical disruption with a bead beater (BioSpec Products). DNA was precipitated and subjected to additional purification with QIAamp mini spin columns (Qiagen).

### 16S rDNA amplification and Illumina Sequencing

For each sample, duplicate 50 μL PCR reactions were performed, each containing 50 ng of purified DNA, 0.2 mmol/L dNTPs, 1.5 mmol/L $MgCl_2$, 2.5 U Platinum Taq DNA polymerase, 2.5 μl of 10× PCR buffer, and 0.5 μM of each primer designed to amplify the V4-V5: 563F (5′-nnnnnnnn-NNNNNNNNNNNN-AYTGGGYDTAAAGNG-3′) and 926R (5′- nnnnnnnn-NNNNNNNNNNNN-CCGTCAATTYHTTTRAGT-3′). A unique 12-base Golay barcode (Ns) precedes the primers for sample identification (23), and 1-8 additional nucleotides were placed in front of the barcode to offset the sequencing of the primers. Cycling conditions were 94°C for 3 minutes, followed by 27 cycles of 94°C for 50 seconds, 51°C for 30 seconds, and 72°C for 1 minute. 72°C for 5 minutes is used for the final

elongation step. Replicate PCRs were pooled, and amplicons were purified using the Qiaquick PCR Purification Kit (Qiagen). PCR products were quantified and pooled at equimolar amounts before Illumina barcodes and adaptors were ligated on using the Illumina TruSeq Sample Preparation protocol. The completed library was sequenced on an Illumina Miseq platform.

Sequence data were compiled and processed using MOTHUR (24). Paired-end read files were converted to standard FASTQ format before being merged. Sequences were grouped into operational taxonomic units (OTUs) using the farthest neighbor algorithm. Sequences with distance-based similarities of 97% or greater were assigned to the same OTU. OTU-based microbial diversity was estimated by calculating the Shannon and Inverse Simpson diversity indices (25). Phylogenetic classification was performed for each sequence, using the Bayesian classifier algorithm described by Wang and colleagues with a bootstrap cutoff of 60% (26). A phylogenetic tree was inferred using Clearcut (27), on the 16S rRNA sequence alignment generated by MOTHUR. Unweighted or weighted UniFrac analysis was carried out using the resulting tree. Principal coordinate analysis (PCoA) was performed on the resulting matrix of distances between each pair of samples.

## Metabolomic analysis

Samples were shipped to Metabolon for detection of metabolites using a database of over 3,000 named molecules. Fecal samples were lyophilized and then resuspended in water (20 μL/mg of dried sample) for homogenization. Following homogenization, 100 μL of the fecal suspensions was used for extraction. Extracts were prepared using the automated MicroLab STAR® system from Hamilton Company. A recovery standard was added prior to the first step in the extraction process for QC purposes. To remove protein, dissociate small molecules bound to protein or trapped in the precipitated protein matrix, and to recover chemically diverse metabolites, proteins were precipitated with methanol under vigorous shaking for 2 minutes followed by centrifugation. The resulting extract was divided into five fractions: one for analysis by UPLC-MS/MS with positive ion mode electrospray ionization, one for analysis by UPLC-MS/MS with negative ion mode electrospray ionization, one for LC polar platform analysis, one for analysis by GC-MS, and one sample was reserved for backup. Samples were placed briefly on a TurboVap® (Zymark) to remove the organic solvent. For LC, the samples were stored overnight under nitrogen before preparation for analysis. For GC, each sample was dried under vacuum overnight before preparation for analysis. Detection of metabolites was performed using Ultrahigh Performance Liquid Chromatography-Tandem Mass Spectroscopy and Gas Chromatography-Mass Spectroscopy (GC-MS) as previously described (28).

## Pathway analysis

Those metabolites with significantly changed levels in feces from celecoxib *vs.* control diet-treated mice were subjected to Ingenuity Pathway Analysis (IPA) software (Winter release 2015; Ingenuity Systems) to determine molecular interactions. KEGG identifiers, Chemical Abstract Service (CAS) registry numbers or human metabolome database identifiers and fold changes were uploaded to IPA and each identifier was mapped to its corresponding metabolite in the IPA Knowledgebase. Interactions were then queried between these

metabolites and diseases or cellular and molecular functions to generate a set of interaction networks. Significantly altered pathways were determined based on the number of molecules altered within a given pathway as determined by the software.

## Immunohistochemistry

Paraffin embedded tissue sections were deparaffinized and incubated with 1% hydrogen peroxide for 20 minutes at room temperature. Sections were subjected to antigen retrieval by boiling in sodium citrate (pH 6.0) then blocked with 10% normal goat serum. Sections were then incubated overnight at 4°C with anti-Ki-67 (1:200; Cell Signaling Technology) antibody. Sections were washed, blocked, incubated with biotinylated anti-rabbit secondary antibody (Vector Laboratories, Inc.) then incubated with avidin-biotin complex reagent (Vector Laboratories, Inc.) for 30 minutes at room temperature, followed by signal detection with 3,3′-diaminobenzidine solution (Vector Laboratories). Tissues were counterstained with hematoxylin.

Cellular proliferation in intestinal crypts was evaluated using Ki-67 immunolabeling. Immunostained sections were assessed for well-oriented crypts with open, straight lumina and a clearly visible base. All of the epithelial cells in the crypt were counted and the percentage of cells that showed nuclear staining for Ki-67 in both basal and non-basal regions was recorded. In the ileum, the crypt base was defined as the deep horizontal portion in which epithelial cells proliferated with their long axes perpendicular to the luminal surface; the lateral aspects of the crypt were considered non-basal regions. For the colon, the crypt base was defined as its deepest aspect as well as the first three cells that extended laterally on each side. For each mouse, an average of 25 and 26 cells were counted in each of 9 crypts of the ileum and colon, respectively. Assessment was independently performed by two authors (E.M.M. and D.C.M) in a blinded fashion with similar results.

## Lgr5 lineage tracing

Nine to 11 week-old *Lgr5-EGFP-ires-CreERT2/Rosa26-lacZ* mice were given control or celecoxib containing diet for 5 weeks then given a single intraperitoneal injection of tamoxifen (Sigma-Aldrich) (160mg/kg). Seven days later, colons and small intestines were harvested and stained for LacZ, using a LacZ Tissue Staining Kit (InvivoGen) and counterstained with hematoxylin solution (Sigma-Aldrich). The extent of lineage tracing was determined in the colon by counting the number of stained cells compared to the total number of cells in a labeled crypt in 3-10 crypts per mouse and reported as a percentage. Quantification in the ileum was carried out by counting the number of marked cells in a labeled crypt and villus compared to the total number of cells in both compartments, in 3-10 crypt/villus units. All quantification was carried out in a blinded manner.

## Statistical analysis

The non-parametric Wilcoxon rank-sum test was used to assess differences between the 2 experimental groups for polyp number and percent of Ki-67 positive cells per crypt. A 2-sample Welch's t-test was used to determine differences in the percent of lineage-traced cells. For metabolomic analysis, biochemicals that were detected in at least 1 sample from each group were analyzed. Missing values for the detected biochemicals were imputed with

the lowest detected value across all groups. Following log transformation, a 3-way (genotype, treatment and time) repeat measure ANOVA was used to estimate the metabolite level under each experimental condition at a given time point. Relevant contrasts were used to assess treatment associated changes at different time points for mice of a certain genotype. A biochemical was considered significantly altered in association with celecoxib treatment if 1) celecoxib led to statistically significant changes at either week 5 or 10 post-treatment compared to baseline and 2) the magnitude of change was statistically significantly greater than the time-dependent change observed in control mice of the same genotype. All statistical tests were two-sided and a p-value $< 0.05$ was considered statistically significant.

## Results

### Celecoxib administration reduces intestinal polyp burden and alters luminal microbiota in *APC*$^{Min/+}$ mice

In order to correlate potential celecoxib-induced changes in the luminal content with reductions in intestinal polyp burden, we first determined the effects of celecoxib on intestinal polyp burden in *APC*$^{Min/+}$ mice. Mice were co-housed from 4 to 6 weeks of age then individually housed and given either AIN-93G diet containing 1000 ppm celecoxib or control diet until 16 weeks of age (Fig. 1A). As shown in Figure 1B and C, celecoxib administration markedly reduced small intestinal polyp number and size in *APC*$^{Min/+}$ mice. In the colon, although there was less than 100% polyp incidence across groups, celecoxib caused a trend in the reduction of polyp number ($0.7 \pm 0.82$ vs. $0.2 \pm 0.42$; $p = 0.139$) and significantly reduced the number of large (≥3mm) polyps ($0.6 \pm 0.7$ vs. $0.0 \pm 0.0$; $p = 0.01$). We next examined whether the microbiota was altered in association with celecoxib-induced polyp reduction. 16S rDNA profiling was carried out to examine bacterial populations on feces collected from the same mice used for polyp quantification at 6, 11 and 16 weeks of age, and ileal content collected at 16 weeks of age. While bacterial profiles did not differ across groups at baseline (data not shown), we found that celecoxib altered bacterial populations in both feces and ileal content from *APC*$^{Min/+}$ mice (Fig. 2A). LefSe analysis revealed that drug treatment decreased the families *Lactobacillaceae* and *Bifidobacteriaceae* in the ileal content and feces, respectively. In contrast, increased *Coriobacteriaceae* was found in both feces and ileal content (Fig. 2B, C).

To determine whether these bacterial changes also occurred in the absence of polyps, we examined the same endpoints in WT mice and again observed a strong celecoxib-induced shift in the microbiota of the ileal content and feces (Fig. 2D). As with *APC*$^{Min/+}$ mice, we found a strong increase in *Coriobacteriaceae* in both ileal content and feces as well as decreased *Bifidobacteriaceae* in feces (Fig. 2E, F). No meaningful changes in diversity were found in mice of either genotype after celecoxib treatment according to the Shannon and Inverse Simpson diversity indices (data not shown).

### The fecal metabolomic profile is altered by celecoxib treatment

Changes in the fecal metabolome can potentially inform on the metabolism of luminal bacteria. Hence, we next determined whether the celecoxib-induced changes in the

microbiota were associated with metabolomic alterations. Targeted metabolomic analysis was carried out on feces from the same $APC^{Min/+}$ and WT mice used for microbiota analysis at 6, 11 and 16 weeks of age. Celecoxib induced a dramatic shift in fecal metabolites regardless of genotype (Fig. 3). The majority of these molecules were decreased (123) while a smaller number increased (26), at either 5 or 10 weeks after initiating treatment of $APC^{Min/+}$ mice. As shown in Figure 4, a large number of amino acids and dipeptides were decreased by celecoxib including glycine, serine and sarcosine. Furthermore, many lipids and nucleotides were also diminished as well as glucose. A similar pattern of metabolomic changes was observed in feces from celecoxib-treated WT mice (Supplementary Fig. S1). Interestingly, many of the small molecules that were diminished in abundance by celecoxib have previously been implicated in the pathogenesis of cancer. For example, deregulated serine and glycine biosynthesis has been shown to impact cancers of the GI tract, lung and breast (29-33).

To gain insight into how these celecoxib-induced metabolomic changes may impact host physiology, we carried out pathway analysis using IPA software. This analysis revealed a large number of changes in the category of “Diseases and Disorders”, in which the top category was “Cancer” (Fig. 5A, left side). Within this category, the top 5 cancers that these metabolites were associated with are of the GI tract (Fig. 5A, right side). Next, we examined how these metabolomic changes were associated with the category of “Molecular and Cellular Functions”. Interestingly, in this category the top function that was affected was “Cellular Growth and Proliferation” in addition to other categories related to cell growth (Fig. 5B, left side). Within the “Cellular Growth and Proliferation” function, we found that the direction of the metabolomic changes induced by celecoxib were overwhelmingly consistent with a reduction in the proliferation of cells (Fig. 5B, right side). We observed a very similar pattern of changes in WT mice (Supplementary Fig. S2). Taken together, we conclude that the pattern of fecal metabolomic changes induced by celecoxib, are consistent with a reduced proliferative state.

## Celecoxib treatment reduces proliferation in the intestinal crypt base

We next determined whether the reduction in proliferation after celecoxib treatment predicted by pathway analysis manifested itself in the host. To assess this possibility, we quantified the proliferation rate in normal appearing ileal crypts of $APC^{Min/+}$ mice given control or celecoxib-containing diet using Ki-67 immunohistochemistry. Upon analysis of the entire crypt, we found a modest but significant reduction in the percentage of Ki-67-positive cells per crypt from those mice given celecoxib compared to controls (Fig. 6A). This observation was largely due to a striking decrease (approximately 50%) in proliferation at the base with no effect on the remainder of the crypt (Fig. 6A, B). We also observed reduced proliferation in the base of normal appearing crypts of the colon (Fig. 6C). In order to determine whether reduced proliferation occurs in biologically normal crypts, Ki-67 IHC analysis was also carried out in ilea and colons of WT littermates given control or celecoxib treatment. As shown in Supplementary Figure S3, drug treatment reduced proliferation in the base of ileal and colon crypts from these mice as well. We next determined whether the celecoxib-induced reduction in proliferating cells in the base of crypts could translate to a diminished ability of stem cells to give rise to the differentiated cells in the crypt. To test

this, we administered control or celecoxib containing diet to *Lgr5-EGFP-ires-CreERT2/Rosa26-lacZ* mice for 5 weeks and then examined the extent of lineage tracing by Lgr5 positive cells over a 7 day period. As shown in Figure 6D-F, celecoxib treatment reduced the ability of Lgr5 positive cells to trace up the crypt by ~40% in both the ileum and colon. There was no difference in the total number of cells per crypt or villus between treatment groups in either organ site (data not shown).

## Discussion

It is thought that celecoxib exerts its chemopreventive effects primarily through inhibition of COX-2. However, it is unknown whether suppression of polyp formation is mediated in part, through changes in the microbiota and/or metabolome. Our data demonstrate that celecoxib treatment alters the luminal microbiota and metabolome in association with suppressing intestinal polyp burden and reducing intestinal stem cell proliferation. The fundamental principle of drug-induced alterations in the microbiota and metabolome leading to reduced intestinal stem cell proliferation may be applicable to the development of other chemopreventive strategies.

As far as we are aware, this study is the first to directly demonstrate that the widely-used NSAID celecoxib can alter the luminal microbiota. Whether these types of effects occur following treatment with other NSAIDs or chemopreventive agents with different mechanisms of action should be evaluated. In fact, recently published work by Liang *et al.*, provides some evidence for this concept by demonstrating that administration of indomethacin to mice induces a shift in the luminal microbiota with a reciprocal effect of the bacteria on drug metabolism (34). Taking into consideration the Liang study as well as the current work, it is possible that several NSAIDs may exert effects on the luminal microbiota, which could explain in part, the chemopreventive efficacy of this class of compounds. If this is the case, then these effects on bacteria may be related to the ability of NSAIDs to inhibit COX-2 in the host leading indirectly to microbial changes or potentially through non-COX-2 mediated effects directly on the bacteria. Ultimately, it will be important to determine whether such an effect occurs in humans given the large percentage of the U.S. population using NSAIDs (35). A retrospective study showing that individuals who have a history of NSAID use have an altered fecal microbial profile suggests this may in fact occur, although a well-controlled prospective clinical study will need to be carried out to definitively answer this question (20).

There is strong evidence that bacterially-derived molecules can impact upon tumorigenesis in the GI tract. These studies have mainly focused on bile acids, short chain fatty acids and polyamines which show both tumor promoting and tumor suppressing effects depending on the particular metabolite (9-13). Similarly, our work raises the possibility that the observed reduction in many growth promoting metabolites in the lumen following celecoxib treatment results from altered metabolism of bacteria. For example, our study revealed associations of bacterial and metabolite changes following celecoxib treatment such as increased *Coriobacteriaceae* and decreased luminal glucose as well as its downstream metabolites serine and glycine. In fact, a causal relationship is supported by previous work demonstrating that increased *Coriobacteriaceae* is associated with reduced hepatic and

systemic glucose levels (36, 37). However, further experiments would need to be carried out to definitively demonstrate that changes in specific bacteria are responsible for select metabolic alterations. Although it is likely that the celecoxib-induced shift in metabolites is a result of changes in bacterial populations and/or metabolism, we appreciate the possibility that the drug may directly alter the metabolome and in turn, induce microbiota changes. Regardless, it is important to note that several of the metabolites whose levels are attenuated by celecoxib treatment, including serine, glycine and nucleotides, can promote cancer cell proliferation (31). Although it is not entirely clear how celecoxib alters the microbiota, it has been suggested that one of the types of bacteria, *coriobacteriaceae* can enhance xenobiotic metabolism which may explain its outgrowth during celecoxib exposure (37). It may also be that certain other bacteria are killed by this drug and in concert outgrowth of other bacteria occurs. Furthermore, it is certainly possible that celecoxib may be indirectly impacting upon luminal bacteria by reducing mucosal $PGE_2$ levels.

We believe that changes in the microbiota and metabolome are likely to help explain why celecoxib inhibits crypt stem cell proliferation potentially contributing to its chemopreventive effects. However, we cannot rule out the possibility that inhibition of COX-2 and reduced $PGE_2$ production may also play a role. The pro-proliferative effects of COX-2 derived $PGE_2$ are well established in the GI tract and COX-2 inhibition by celecoxib and other NSAIDs has been shown to reduce epithelial proliferation (38). Although COX-2 is not expressed in most cells within the normal GI tract, it is expressed in tuft cells, a small population of cells found in the normal murine small intestine (39). Therefore, it is possible that celecoxib will inhibit COX-2 in this cell type or possibly other cell types leading to reduced stem cell proliferation. Furthermore the possibility that celecoxib may act directly on stem cells cannot be excluded.

Stem cells are believed to play an important role in the etiology of many cancers and contribute to therapeutic resistance (40, 41). In the GI tract, stem cells were shown to be a critical cell-of-origin for intestinal polyp development through loss of *Apc* (42). Interestingly, our data show that celecoxib-induced alterations in the microbiota and metabolome are associated with decreased proliferation selectively in the base of ileal and colonic crypts, where stem cells are found (Fig. 6A-C). Furthermore, our results showing a reduced ability of Lgr5-positive cells to lineage trace up the crypt following celecoxib treatment is consistent with a reduced proliferative capacity of stem cells (Fig. 6D-F). Taken together, we believe that the reduction in stem cell proliferation is likely to contribute to the observed decrease in polyp formation in celecoxib treated $APC^{Min/+}$ mice. Importantly, our study fits with other recent evidence that exogenous factors, e.g., diet can modulate GI stem cell proliferation (43, 44).

Although there are several interesting observations in this study, there are also some limitations. The pathway analysis results produced by IPA software are limited by the robustness of the algorithms used and the number of metabolites in its database. As the field of metabolomic analysis matures such findings may evolve to include alternative or additional pathways. Additionally, the possibility that celecoxib may be mediating these effects through suppressing prostaglandin production was not explored. Whether similar celecoxib-induced changes in the microbiota, metabolome and epithelium occur in the

normal intestinal tissue of *Cox-2* knockout mice or whether administration of $PGE_2$ or activation of EP receptor signaling reverses the observed effects could be explored to evaluate this point. $APC^{Min/+}$ mice are a well-established model to study the chemopreventive effects of NSAIDs. However, this model has certain limitations given the propensity to develop polyps in the small intestine. Moreover, the polyps do not progress to cancer. Other more relevant models should be explored to determine whether similar effects occur after celecoxib treatment including mice with *Apc* mutations in combination with alterations in *p53* or *Kras* as well as more newly developed models that have a greater propensity to develop colon tumors (45, 46). Our group attempted to carry out similar work in the azoxymethane model but was unsuccessful due to toxicity resulting from the combination of carcinogen and celecoxib (unpublished).

Taken together, our data raise the possibility that the chemopreventive activity of celecoxib can be explained, in part, by its effects on the microbiota and their metabolites leading to reduced epithelial cell proliferation. Our study highlights the possibility of targeting the microbiota or metabolome as a timely new strategy to decrease cancer risk.

## Supplementary Material

Refer to Web version on PubMed Central for supplementary material.

## Acknowledgments

The authors thank Dr. Peter Holt for numerous helpful discussions.

**Grant Support:** The project was supported by NIH/NCATS TL1 TR000459 (D.C. Montrose), NIH/NCI contract HHSN2612012000181 (A.J. Dannenberg & S.S. Gross) and the New York Crohn's Foundation (A.J. Dannenberg).

## References

1. Sears CL, Garrett WS. Microbes, microbiota, and colon cancer. Cell Host Microbe. 2014; 15:317–28. [PubMed: 24629338]
2. Marchesi JR, Dutilh BE, Hall N, Peters WH, Roelofs R, Boleij A, et al. Towards the human colorectal cancer microbiome. PLoS One. 2011; 6:e20447. [PubMed: 21647227]
3. Sobhani I, Tap J, Roudot-Thoraval F, Roperch JP, Letulle S, Langella P, et al. Microbial dysbiosis in colorectal cancer (CRC) patients. PLoS One. 2011; 6:e16393. [PubMed: 21297998]
4. Arthur JC, Perez-Chanona E, Muhlbauer M, Tomkovich S, Uronis JM, Fan TJ, et al. Intestinal inflammation targets cancer-inducing activity of the microbiota. Science. 2012; 338:120–3. [PubMed: 22903521]
5. Kostic AD, Chun E, Robertson L, Glickman JN, Gallini CA, Michaud M, et al. Fusobacterium nucleatum potentiates intestinal tumorigenesis and modulates the tumor-immune microenvironment. Cell Host Microbe. 2013; 14:207–15. [PubMed: 23954159]
6. Wu S, Rhee KJ, Albesiano E, Rabizadeh S, Wu X, Yen HR, et al. A human colonic commensal promotes colon tumorigenesis via activation of T helper type 17 T cell responses. Nat Med. 2009; 15:1016–22. [PubMed: 19701202]
7. Bongers G, Pacer ME, Geraldino TH, Chen L, He Z, Hashimoto D, et al. Interplay of host microbiota, genetic perturbations, and inflammation promotes local development of intestinal neoplasms in mice. J Exp Med. 2014; 211:457–72. [PubMed: 24590763]
8. Garrett WS, Punit S, Gallini CA, Michaud M, Zhang D, Sigrist KS, et al. Colitis-associated colorectal cancer driven by T-bet deficiency in dendritic cells. Cancer Cell. 2009; 16:208–19. [PubMed: 19732721]

9. Babbar N, Gerner EW. Targeting polyamines and inflammation for cancer prevention. Recent Results Cancer Res. 2011; 188:49–64. [PubMed: 21253788]
10. Bernstein H, Bernstein C, Payne CM, Dvorakova K, Garewal H. Bile acids as carcinogens in human gastrointestinal cancers. Mutat Res. 2005; 589:47–65. [PubMed: 15652226]
11. Johnson CH, Dejea CM, Edler D, Hoang LT, Santidrian AF, Felding BH, et al. Metabolism links bacterial biofilms and colon carcinogenesis. Cell Metab. 2015; 21:891–7. [PubMed: 25959674]
12. Scharlau D, Borowicki A, Habermann N, Hofmann T, Klenow S, Miene C, et al. Mechanisms of primary cancer prevention by butyrate and other products formed during gut flora-mediated fermentation of dietary fibre. Mutat Res. 2009; 682:39–53. [PubMed: 19383551]
13. Belcheva A, Irrazabal T, Robertson SJ, Streutker C, Maughan H, Rubino S, et al. Gut microbial metabolism drives transformation of MSH2-deficient colon epithelial cells. Cell. 2014; 158:288–99. [PubMed: 25036629]
14. Montrose DC, Zhou XK, Kopelovich L, Yantiss RK, Karoly ED, Subbaramaiah K, et al. Metabolic profiling, a noninvasive approach for the detection of experimental colorectal neoplasia. Cancer Prev Res (Phila). 2012; 5:1358–67. [PubMed: 22961778]
15. Steinbach G, Lynch PM, Phillips RK, Wallace MH, Hawk E, Gordon GB, et al. The effect of celecoxib, a cyclooxygenase-2 inhibitor, in familial adenomatous polyposis. N Engl J Med. 2000; 342:1946–52. [PubMed: 10874062]
16. Bertagnolli MM, Eagle CJ, Zauber AG, Redston M, Solomon SD, Kim K, et al. Celecoxib for the prevention of sporadic colorectal adenomas. N Engl J Med. 2006; 355:873–84. [PubMed: 16943400]
17. Jacoby RF, Seibert K, Cole CE, Kelloff G, Lubet RA. The cyclooxygenase-2 inhibitor celecoxib is a potent preventive and therapeutic agent in the min mouse model of adenomatous polyposis. Cancer Res. 2000; 60:5040–4. [PubMed: 11016626]
18. Syer SD, Wallace JL. Environmental and NSAID-enteropathy: dysbiosis as a common factor. Curr Gastroenterol Rep. 2014; 16:377. [PubMed: 24532193]
19. Uejima M, Kinouchi T, Kataoka K, Hiraoka I, Ohnishi Y. Role of intestinal bacteria in ileal ulcer formation in rats treated with a nonsteroidal antiinflammatory drug. Microbiol Immunol. 1996; 40:553–60. [PubMed: 8887349]
20. Rogers MA, Aronoff DM. The influence of non-steroidal anti-inflammatory drugs on the gut microbiome. Clin Microbiol Infect. 2016; 22:178 e1–9. [PubMed: 26482265]
21. Chiu HC, Yang J, Soni S, Kulp SK, Gunn JS, Schlesinger LS, et al. Pharmacological exploitation of an off-target antibacterial effect of the cyclooxygenase-2 inhibitor celecoxib against Francisella tularensis. Antimicrob Agents Chemother. 2009; 53:2998–3002. [PubMed: 19398640]
22. Thangamani S, Younis W, Seleem MN. Repurposing celecoxib as a topical antimicrobial agent. Front Microbiol. 2015; 6:750. [PubMed: 26284040]
23. Caporaso JG, Lauber CL, Walters WA, Berg-Lyons D, Huntley J, Fierer N, et al. Ultra-high-throughput microbial community analysis on the Illumina HiSeq and MiSeq platforms. ISME J. 2012; 6:1621–4. [PubMed: 22402401]
24. Schloss PD, Westcott SL, Ryabin T, Hall JR, Hartmann M, Hollister EB, et al. Introducing mothur: open-source, platform-independent, community-supported software for describing and comparing microbial communities. Appl Environ Microbiol. 2009; 75:7537–41. [PubMed: 19801464]
25. Buckland ST, Magurran AE, Green RE, Fewster RM. Monitoring change in biodiversity through composite indices. Philos Trans R Soc Lond B Biol Sci. 2005; 360:243–54. [PubMed: 15814343]
26. Wang M, Chen Z, Cloutier S. A hybrid Bayesian network learning method for constructing gene networks. Comput Biol Chem. 2007; 31:361–72. [PubMed: 17889617]
27. Sheneman L, Evans J, Foster JA. Clearcut: a fast implementation of relaxed neighbor joining. Bioinformatics. 2006; 22:2823–4. [PubMed: 16982706]
28. Evans A, Bridgewater B, Liu Q, Mitchell M, Robinson R, Dai H, et al. High Resolution Mass Spectrometry Improves Data Quantity and Quality as Compared to Unit Mass Resolution Mass Spectrometry in High-Throughput Profiling Metabolomics. Metabolomics. 2014; 4:7.
29. DeNicola GM, Chen PH, Mullarky E, Sudderth JA, Hu Z, Wu D, et al. NRF2 regulates serine biosynthesis in non-small cell lung cancer. Nat Genet. 2015; 47:1475–81. [PubMed: 26482881]

30. Hirayama A, Kami K, Sugimoto M, Sugawara M, Toki N, Onozuka H, et al. Quantitative metabolome profiling of colon and stomach cancer microenvironment by capillary electrophoresis time-of-flight mass spectrometry. Cancer Res. 2009; 69:4918–25. [PubMed: 19458066]
31. Locasale JW. Serine, glycine and one-carbon units: cancer metabolism in full circle. Nat Rev Cancer. 2013; 13:572–83. [PubMed: 23822983]
32. Locasale JW, Grassian AR, Melman T, Lyssiotis CA, Mattaini KR, Bass AJ, et al. Phosphoglycerate dehydrogenase diverts glycolytic flux and contributes to oncogenesis. Nat Genet. 2011; 43:869–74. [PubMed: 21804546]
33. Possemato R, Marks KM, Shaul YD, Pacold ME, Kim D, Birsoy K, et al. Functional genomics reveal that the serine synthesis pathway is essential in breast cancer. Nature. 2011; 476:346–50. [PubMed: 21760589]
34. Liang X, Bittinger K, Li X, Abernethy DR, Bushman FD, FitzGerald GA. Bidirectional interactions between indomethacin and the murine intestinal microbiota. Elife. 2015:4.
35. Paulose-Ram R, Hirsch R, Dillon C, Losonczy K, Cooper M, Ostchega Y. Prescription and non-prescription analgesic use among the US adult population: results from the third National Health and Nutrition Examination Survey (NHANES III). Pharmacoepidemiol Drug Saf. 2003; 12:315–26. [PubMed: 12812012]
36. Bangsgaard Bendtsen KM, Krych L, Sorensen DB, Pang W, Nielsen DS, Josefsen K, et al. Gut microbiota composition is correlated to grid floor induced stress and behavior in the BALB/c mouse. PLoS One. 2012; 7:e46231. [PubMed: 23056268]
37. Claus SP, Ellero SL, Berger B, Krause L, Bruttin A, Molina J, et al. Colonization-induced host-gut microbial metabolic interaction. MBio. 2011; 2:e00271–10. [PubMed: 21363910]
38. Simmons DL, Botting RM, Hla T. Cyclooxygenase isozymes: the biology of prostaglandin synthesis and inhibition. Pharmacol Rev. 2004; 56:387–437. [PubMed: 15317910]
39. Bezencon C, Furholz A, Raymond F, Mansourian R, Metairon S, Le Coutre J, et al. Murine intestinal cells expressing Trpm5 are mostly brush cells and express markers of neuronal and inflammatory cells. J Comp Neurol. 2008; 509:514–25. [PubMed: 18537122]
40. Muller M, Hermann PC, Liebau S, Weidgang C, Seufferlein T, Kleger A, et al. The role of pluripotency factors to drive stemness in gastrointestinal cancer. Stem Cell Res. 2016; 16:349–57. [PubMed: 26896855]
41. Zhao J. Cancer stem cells and chemoresistance: The smartest survives the raid. Pharmacol Ther. 2016; 160:145–58. [PubMed: 26899500]
42. Barker N, Ridgway RA, van Es JH, van de Wetering M, Begthel H, van den Born M, et al. Crypt stem cells as the cells-of-origin of intestinal cancer. Nature. 2009; 457:608–11. [PubMed: 19092804]
43. Beyaz S, Mana MD, Roper J, Kedrin D, Saadatpour A, Hong SJ, et al. High-fat diet enhances stemness and tumorigenicity of intestinal progenitors. Nature. 2016; 531:53–8. [PubMed: 26935695]
44. Peregrina K, Houston M, Daroqui C, Dhima E, Sellers RS, Augenlicht LH. Vitamin D is a determinant of mouse intestinal Lgr5 stem cell functions. Carcinogenesis. 2015; 36:25–31. [PubMed: 25344836]
45. Dow LE, O'Rourke KP, Simon J, Tschaharganeh DF, van Es JH, Clevers H, et al. Apc Restoration Promotes Cellular Differentiation and Reestablishes Crypt Homeostasis in Colorectal Cancer. Cell. 2015; 161:1539–52. [PubMed: 26091037]
46. Jackstadt R, Sansom OJ. Mouse models of intestinal cancer. J Pathol. 2016; 238:141–51. [PubMed: 26414675]

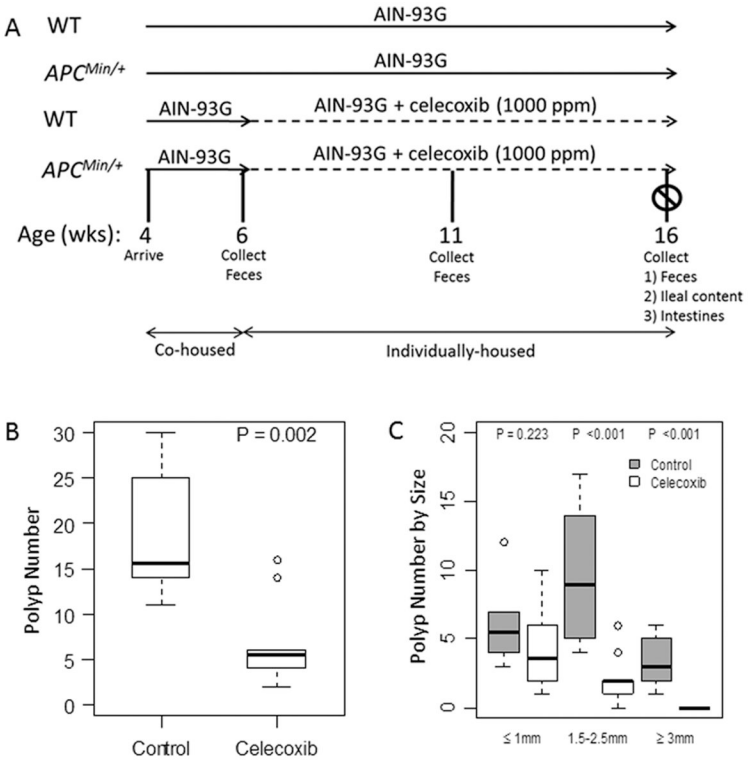


**Figure 1.**

Celecoxib reduces intestinal polyp burden in *APC*$^{Min/+}$ mice. A, Schematic representation of experimental design. B-C, Polyp number (B) and size (C) were determined in the small intestines of *APC*$^{Min/+}$ mice given control or celecoxib containing diet. (n=10 per group).

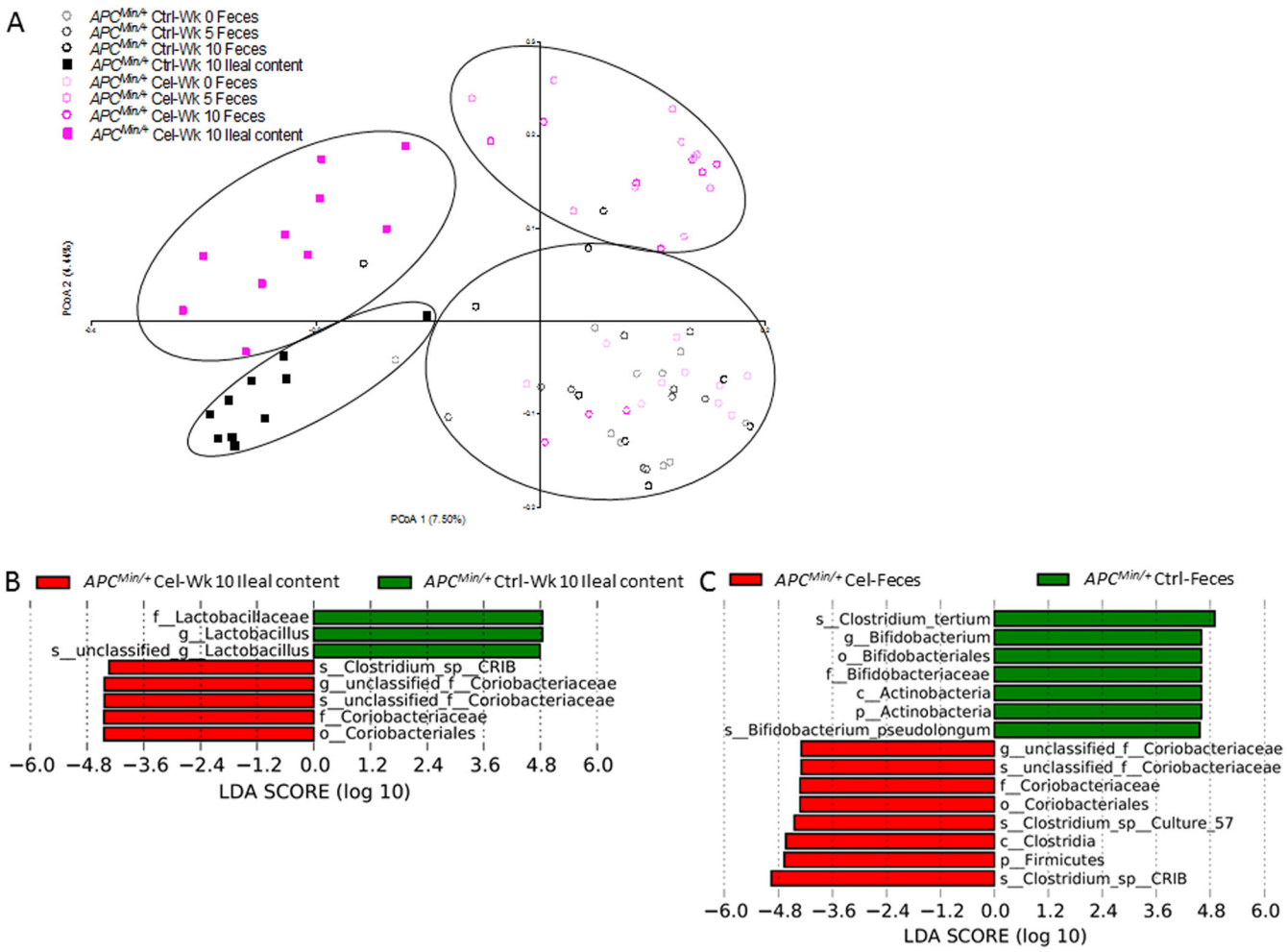

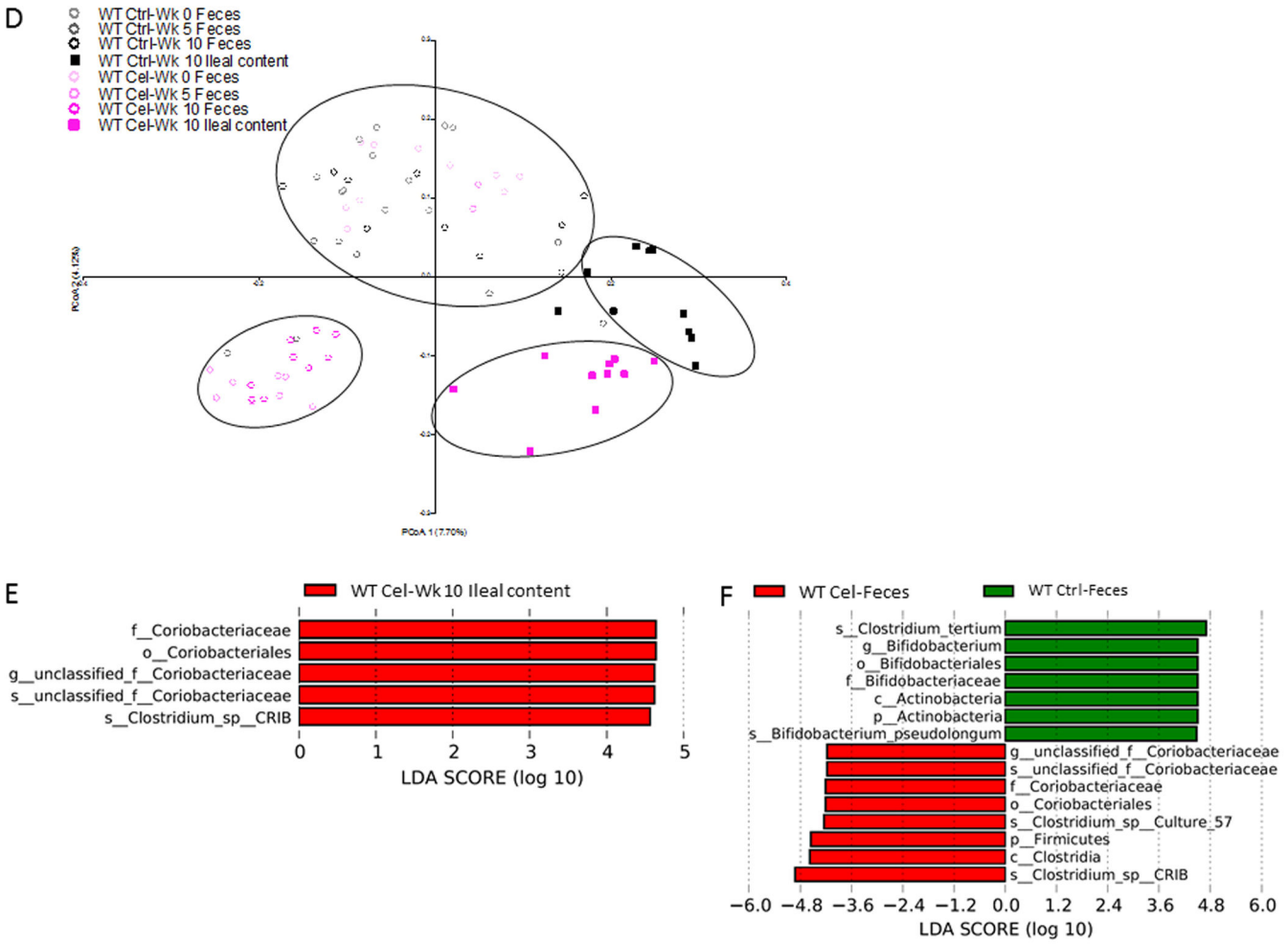


**Figure 2.**

Celecoxib treatment alters the luminal microbiota in *APC*$^{Min/+}$ mice. A, Principal component analysis results of 16S rDNA sequencing of ileal content and feces from *APC*$^{Min/+}$ mice given control or celecoxib diet. Black circles indicate those groups that cluster together. LefSe analysis was carried out on sequencing results from the ileal content (B) and feces (C) to determine which bacterial populations differed between treatment groups. D-F, Principal component analysis results of 16S rDNA sequencing (D) and LefSe analysis of ileal content (E) and feces (F) from WT mice are shown.

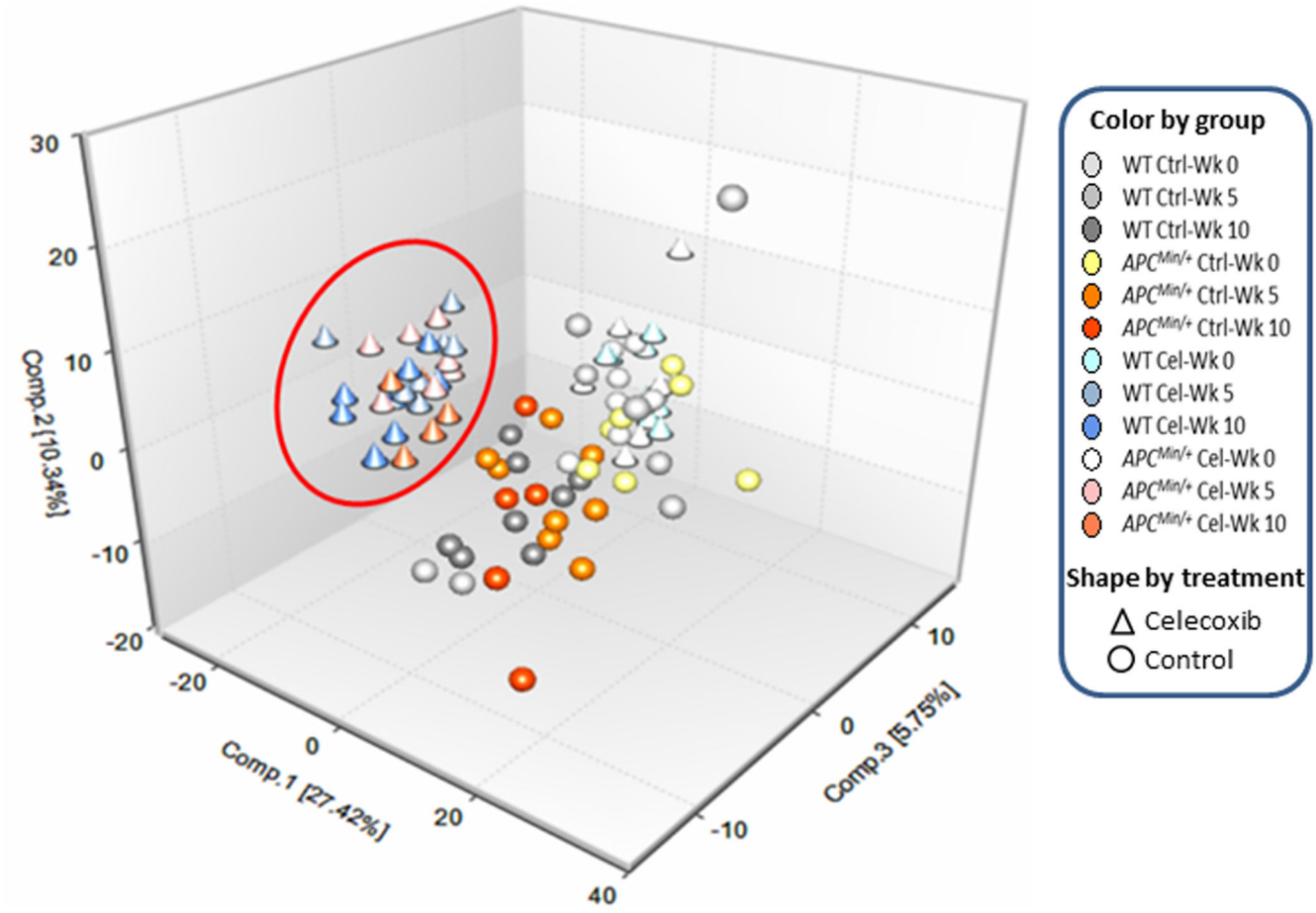


**Figure 3.**

Fecal metabolites are altered by celecoxib in *APC*$^{Min/+}$ and WT mice. Principal component analysis was carried out on data generated by targeted metabolomics of feces from control or celecoxib-treated mice. Symbols inside the red circle indicate those mice given celecoxib for 5 or 10 weeks. Symbols outside of the red circle represent mice that received control diet. Each group of mice (genotype, treatment or time point) is represented by a different color (Color by group). Those mice given control diet are represented by circles while celecoxib treated mice are represented by cone-shaped symbols, regardless of genotype (Shape by treatment).

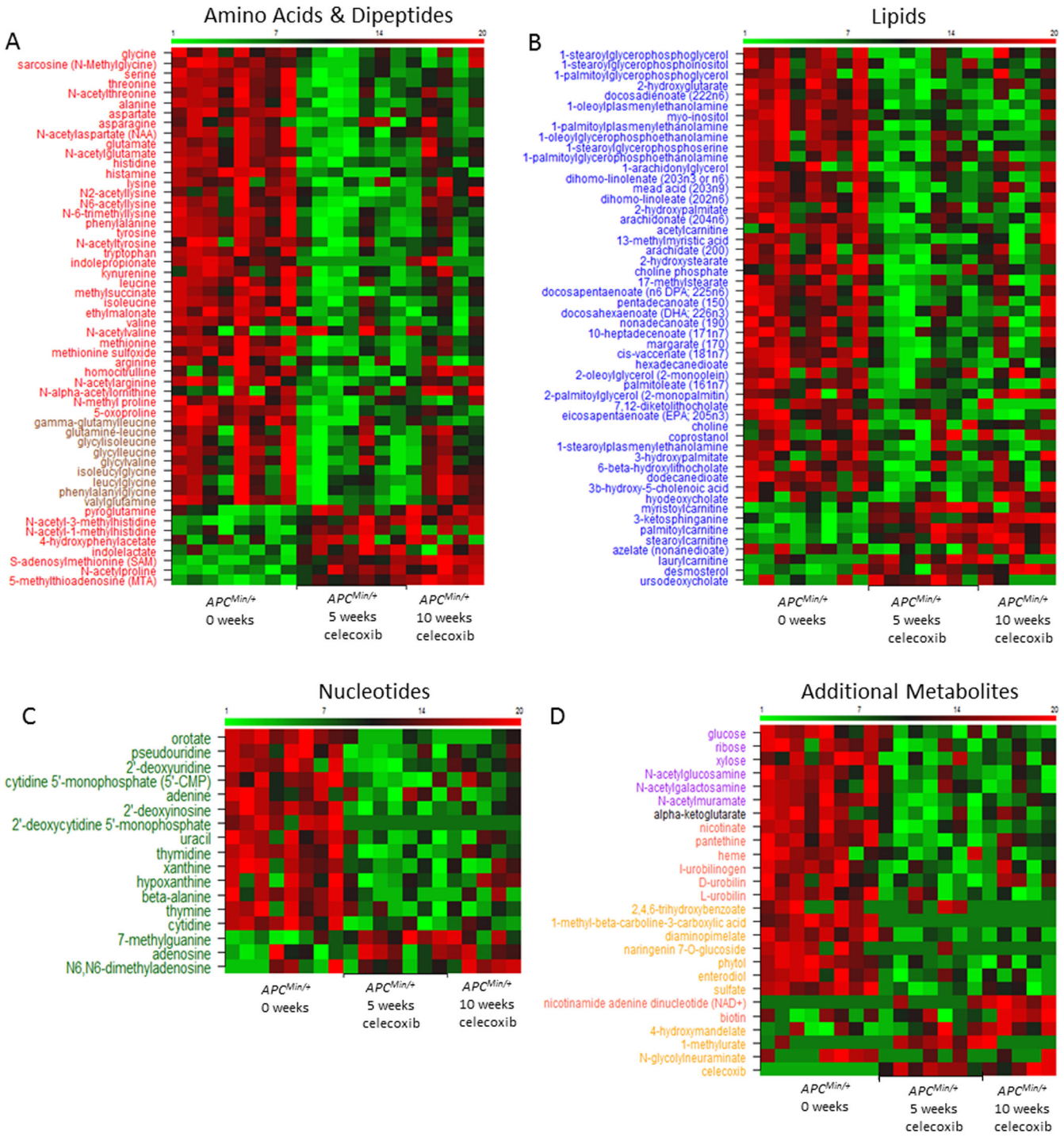


**Figure 4.**

Administration of celecoxib alters the luminal metabolome of *APC*$^{Min/+}$ mice. Heat maps of significantly altered metabolites were generated by comparing the metabolite changes of feces from *APC*$^{Min/+}$ mice given celecoxib to *APC*$^{Min/+}$ mice given control diet. A, Amino acids and Dipeptides. B, Lipids. C, Nucleotides. D, Additional Metabolites. Each column represents an individual sample. Data are rank transformed and displayed as color intensity

with low levels indicated by green color and high levels indicated by red color. Metabolites in different metabolic pathways are color coded as follows: Red font = amino acid, brown font = dipeptides, dark blue font = lipids, green font = nucleotides, purple font = carbohydrates, light red font = cofactors and vitamins, black font = energy and orange font = xenobiotics. The metabolite categories described above were broadly defined to include related metabolites.

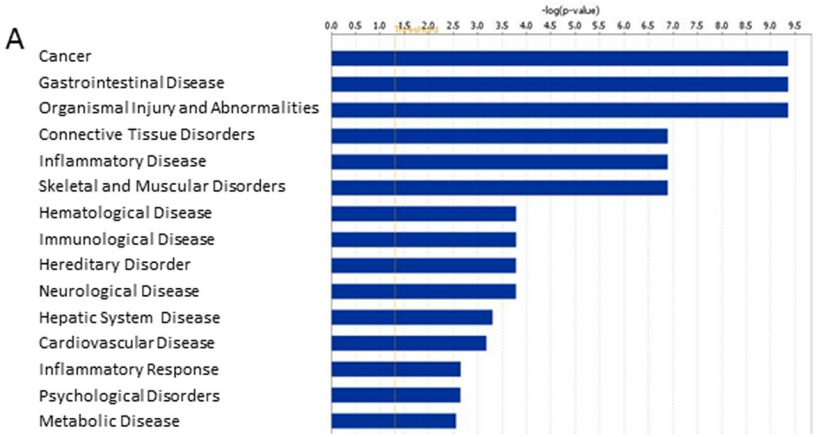


| Diseases or Functions Annotation | p-Value |
|---|---|
| gastroesophageal cancer | 4.39E-10 |
| colon cancer | 4.69E-10 |
| gastric cancer | 5.48E-10 |
| stomach tumor | 1.52E-09 |
| colorectal cancer | 8.60E-09 |

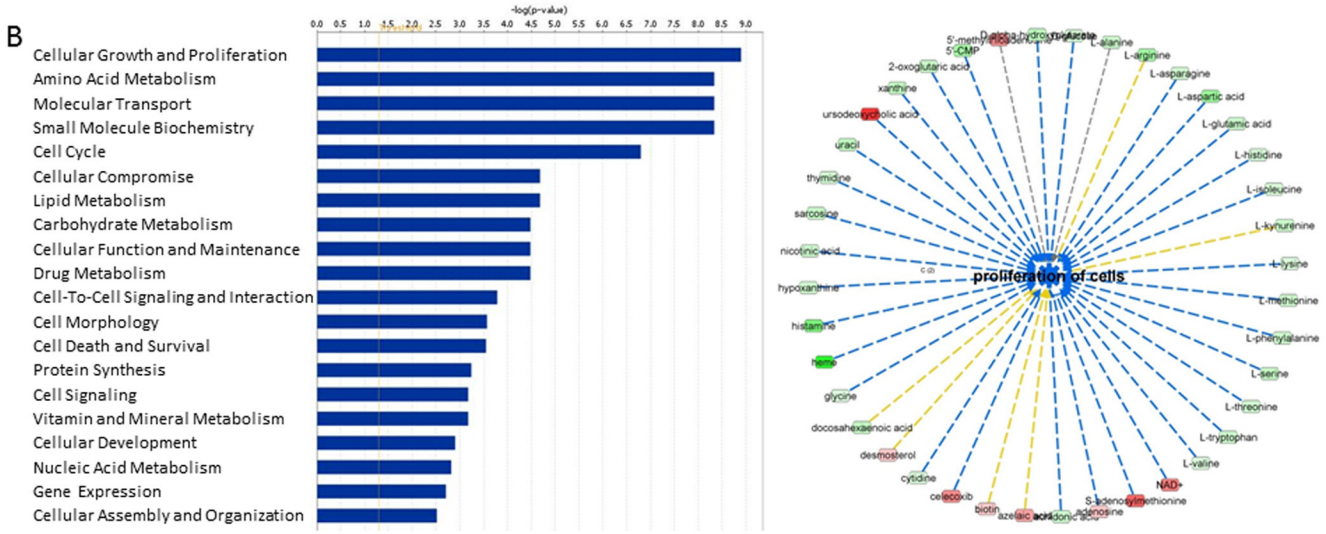


**Figure 5.**

Pathway alterations associated with celecoxib-induced metabolite changes in $APC^{Min/+}$ mice. The metabolomic changes induced by celecoxib treatment in $APC^{Min/+}$ mice were analyzed by Ingenuity Pathway Analysis. A, The top 15 diseases that were significantly associated with the altered metabolites are shown (left side). Blue bars represent the -log p-value and the threshold represents a p-value which equals 0.05. The “Cancer” category was further defined by type which revealed the top five significantly associated types of cancer (right side). B, The top 20 cellular and molecular functions that are significantly associated with the changes in metabolites are shown (left side). The “Cellular Growth and Proliferation” category was further analyzed to show that the direction of change (red = increased; green = decreased; color intensity reflects magnitude of change) in the majority of metabolites corresponded to decreased proliferation of cells (right side). Blue dashed line = predicted inhibition; yellow dashed line = findings inconsistent with state of downstream molecule; gray dashed line = effect not predicted.

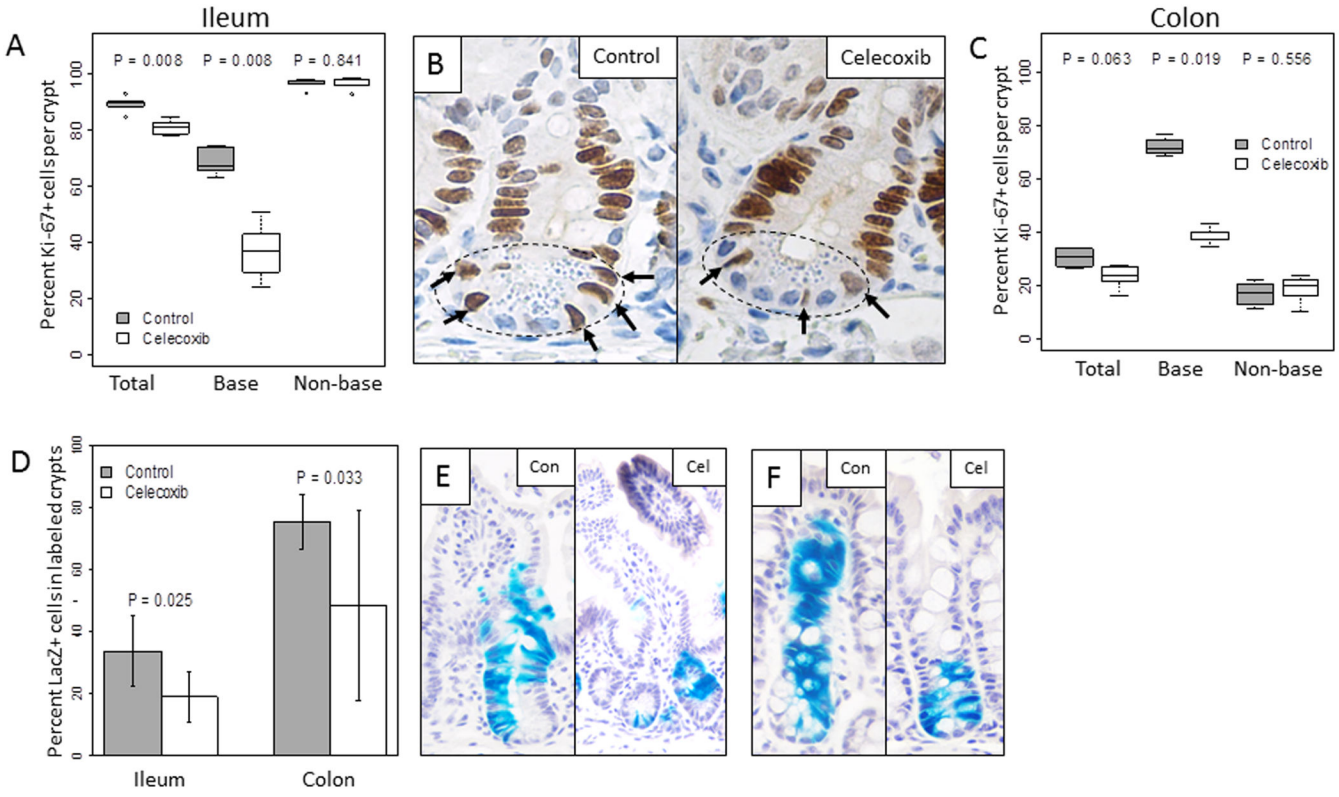


**Figure 6.**

Celecoxib treatment reduces proliferation in the base of normal appearing crypts from *APC*$^{Min/+}$ mice. A, The percent of Ki-67 positive cells in the entire crypt, base and non-base were quantified in the ilea of *APC*$^{Min/+}$ mice given control or celecoxib diet. Data are reported as median (n = 5 per group). . B, Representative images of Ki-67 stained crypts from control or celecoxib-treated mice are shown. Dashed circle indicates the base of the crypt; arrows indicate positively stained cells. C, The percent of Ki-67 positive cells in the entire crypt, base and non-base were quantified in colonic crypts from *APC*$^{Min/+}$ mice given control or celecoxib diet. D, The percent of cells stained positively for LacZ in ilea and colons of *Lgr5-EGFP-ires-CreERT2/Rosa26-lacZ* mice given control or celecoxib diet are shown. Data are summarized using mean ± SD (n = 3 to 4 per group). E-F, Representative images of LacZ staining in ilea (E) and colons (F) of control or celecoxib-treated *Lgr5-EGFP-ires-CreERT2/Rosa26-lacZ* mice.